



Gas Evolution on Graphite and Oxygen Evolving Anodes During Aluminium Electrolysis

Laurent Cassayre, Gabriel Plascencia, T. Marin, S. Fan, Torstein A. Utigard

► To cite this version:

Laurent Cassayre, Gabriel Plascencia, T. Marin, S. Fan, Torstein A. Utigard. Gas Evolution on Graphite and Oxygen Evolving Anodes During Aluminium Electrolysis. Annual meeting of The Minerals, Metals & Materials Society, Mar 2006, San Antonio, United States. pp.0. hal-04105798

HAL Id: hal-04105798

<https://hal.science/hal-04105798>

Submitted on 25 May 2023

HAL is a multi-disciplinary open access archive for the deposit and dissemination of scientific research documents, whether they are published or not. The documents may come from teaching and research institutions in France or abroad, or from public or private research centers.

L'archive ouverte pluridisciplinaire **HAL**, est destinée au dépôt et à la diffusion de documents scientifiques de niveau recherche, publiés ou non, émanant des établissements d'enseignement et de recherche français ou étrangers, des laboratoires publics ou privés.

GAS EVOLUTION ON GRAPHITE AND OXYGEN-EVOLVING ANODES DURING ALUMINIUM ELECTROLYSIS

L. Cassayre¹, G. Plascencia², T. Marin³, S. Fan⁴ and T. Utigard⁴

¹Joint Research Centre, Institute of Transuranium Elements, P.O. Box 2340, 76125 Karlsruhe, Germany

²CIITEC – IPN, Mexico City, Mexico

³Department of Mines, Faculty of Engineering, University of Chile, Santiago, Chile

⁴Materials Science and Engineering, University of Toronto, 184 College Street, Toronto, ON, Canada M5S 3E4

Keywords: aluminium electrolysis, gas evolution, slotted anode, inert anode

Abstract

Anode gas evolution, growth and flow behaviour during aluminium electrolysis have been investigated using various experimental techniques, including water modelling, X-ray visualization and direct observation. Video recordings of oxygen-evolving anodes (SnO₂, Cu, Cu-Ni) and carbon anodes were performed in laboratory electrolysis cells of various scales. The water model also investigated the effects of slotted anodes on the gas escape from beneath large anodes. Beneath large horizontal anodes, individual bubbles form and are then subsequently swept away by large sweeping bubbles flowing rapidly beneath the bottom surface. The gas behaviour on oxygen evolving anodes was very different from that with carbon, with the formation of very small bubbles that released very quickly from the anode due to improved wetting of the anode by the electrolyte.

Introduction

In the Hall-Héroult process, aluminium is produced by electrolysis of alumina at 960 °C. The cell contains normally 15 to 20 cm of liquid aluminium which also acts as the cathode. Carbon anodes are suspended in the cryolite based electrolyte and separated from the aluminium pool by a distance of 4 to 5 cm. Modern cells with cell currents above 250 kA are capable of producing aluminium at 13-14 kWh/kg of aluminium and with a current efficiency of 95-97%. These cells represent major improvements in technology over the last two decades. These advancements are based on extensive theoretical and mathematical studies, laboratory and plant investigations, and plant operating experience. However, most of these investigations are based on indirect measurements since very little of what actually takes place within the cell can be observed. To “look” into the process, we have developed various techniques to visualize the gas evolution, including both wetting characteristics and flow behaviour beneath the anodes [1, 2].

The two main objectives of this work were to investigate the effect of slots in the anodes on the gas escape behaviour and to study the gas behaviour using inert anodes. With the use of large anodes, the gas escape from beneath such large horizontal surfaces may lead to excessive electrolyte stirring as well as increased anode voltages due to the large surface coverage by gas bubbles. Slotted anodes have recently been introduced to allow easier gas escape. The use of inert anodes is likely to affect gas evolution and flow behaviour. One aim of the current work was to compare the gas behaviour between oxygen evolving and graphite anodes, and to characterize the bubble size and the bubble layer depth in the inter-electrode area.

While various materials have already been patented for inert anode application, none is yet in commercial use [3]. This is mainly because the severe operating environment and the need of good electronic conductivity limit the number of suitable materials. Most recent research has concentrated on metals, oxide ceramics and cermets. In the present study, copper, copper-nickel alloy (wt% 75/25) and tin oxide materials were tested as oxygen-evolving anodes, even if none of them is stable enough to totally resist to corrosion.

Video recordings of electrolysis at various current densities (CD) were performed in laboratory cells, using direct observation from above, see-through cell and radiography techniques [4,5]. The influence of the alumina content in the electrolyte was studied for graphite and tin-oxide. A comparison of the wettability of the materials by the electrolyte was also carried out to try to explain the very different gas behaviour observed.

Experimental Techniques

The experimental techniques used include: Direct observations from above, Quartz see through cell, X-ray radiography, Hot-thermocouple microscope, Hot-stage microscope and Water-modelling.

Direct Observations From Above

Experiments were carried out in graphite crucibles with 1.5 kg of cryolite and placed inside an inconel container and heated inside a furnace (Fig. 1A). The voltage measurements were made directly from the stainless steel buss bars holding the anode and the cathode (crucible). Anode vertical positioning was achieved via a screw-driven linear movement device. The current and voltage signals were transmitted to isolated inputs of the data acquisition. The graphite (Union Carbide AGSR grade) used to make the anodes had a density of approx. 1.7 g/cm³.

Quartz See Through Cell (Fig. 1B)

Electrolysis was also carried out in transparent quartz tubes (Ø=54 mm) placed in an electric furnace allowing lateral observations through a hole in the front panel, as described by Haupin et al. [6]. In this see-through cell, the cathode was a graphite cylinder (Ø=43 mm, h=15 mm) located at the bottom of the tube, and the anode was a graphite or tin-oxide cylinder (Ø=9 mm, h=50 mm), vertically positioned 2 cm above the cathode. A new quartz tube was used for each experiment.

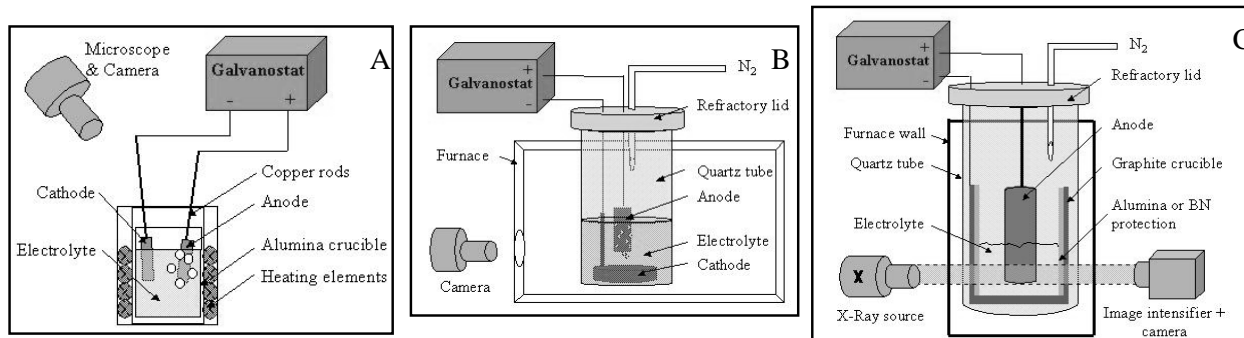


Figure 1: Schematics of the experimental conditions
A: Observation from above B: See-through cell C: X-Ray furnace

Two different electrolyte compositions were used, based on a mixture of cryolite with AlF_3 (11 wt%), CaF_2 (5 wt%) and Al_2O_3 . Weight fraction of alumina was either 2.5 wt% (electrolyte A) or 9 wt% (electrolyte B), electrolyte B being saturated in alumina. The mix of powders was pre-melted at 1000°C in graphite crucibles, then cast, crushed and stored dry.

X-ray Radiography (Fig. 1C)

The experiments were carried out in graphite crucibles with inner diameters from 17 to 23 mm with 2 to 9 mm graphite or inert anodes. Images of the aluminium drop and the graphite anode immersed in the electrolyte were formed on a photographic film by a horizontal beam of X-rays. Gas bubbles appear white because they allow X-rays to pass through. More dense materials such as aluminium, appears darker. The experiments were recorded using a TV camera-monitor and a video recorder.

Hot-thermocouple Microscope

A hot-thermocouple method was employed in conjunction with a microscope and a video camera. A very small sample (0.5 g) of electrolyte was attached to and heated by passing current through a Pt/Pt-Rh thermocouple. A pair of platinum electrodes (0.3 mm dia.) was inserted in the sample after melting and electrolysis was initiated and observed using a microscope.

Hot-stage Microscope

A 'hot-stage microscope' was developed in order to allow for bigger samples than what could be achieved by the hot-thermocouple method. A 1-3 g sample of cryolite was placed on a boat and heated by a platinum foil and contained in a gas-tight Pyrex container. A pair of graphite electrodes (1-1.3 mm dia.) and a thermocouple could be placed within the sample. A microscope was used to monitor the various phenomena taking place.

Water-modelling

The water model was constructed from acrylic plastic. The purpose of this technique was to study the gas behaviour beneath large horizontal, sloped and slotted anodes. The model represents half of an anode which is suspended inside a tank and can be moved relative to the cathode. Three independent chambers in the anode can be pressurized with gas to force bubbles to form on the face of the brass sheet. The entire model is situated on top of two

scissor jacks which allows the angle of the cathode and anode to be adjusted.

Bubbling at Graphite Anodes

At current densities below 0.2 A/cm^2 , bubble birth occurs on specific nucleation spots on the graphite anode. Increasing CD leads to a large number of nucleation sites. Round-shaped bubbles grow and coalesce until reaching 2-3 mm in diameter, then detach and escape vertically. As shown on Figure 2, the surface coverage of the anode is very high and the small bubbles appears stuck to the anode.

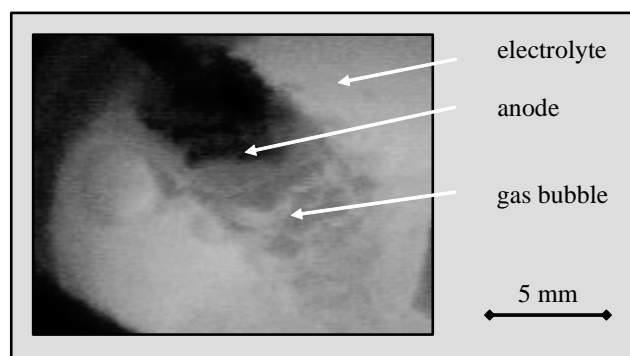


Figure 2: Observation from above - side bubbles on graphite anode [$\varnothing_{\text{anode}}=5\text{mm}$, $\text{CD}=0.2 \text{ A.cm}^{-2}$, $T=960^\circ\text{C}$, 9% Al_2O_3]

Tests in the quartz see-through cell were limited to less than 7 minutes and CD up to 0.5 A/cm^2 , because streamers rapidly arose in the cell and lead to an opaque electrolyte. It was observed that the anode gas was released periodically. At small CDs (up to around 0.5 A/cm^2), several bubbles form on the bottom surface of the anode, then grow and coalesce until a single large bubble covers the whole area and is finally released, leaving a clean surface free of gas. Figure 3 shows a bubble trapped under the anode just before release, during see-through cell electrolysis at 0.2 A/cm^2 .

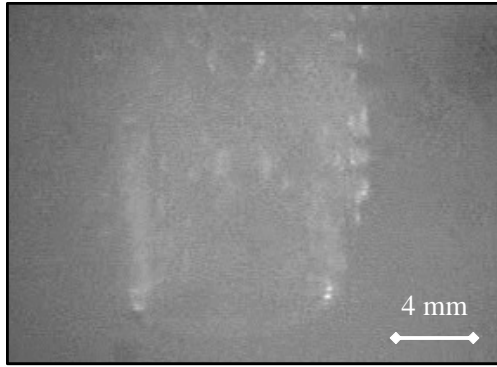


Figure 3: Graphite anode during electrolysis in see-through cell [$\varnothing_{\text{anode}}=9\text{mm}$, $\text{CD}=0.2 \text{ A/cm}^2$, $T=960^\circ\text{C}$, $9\% \text{ Al}_2\text{O}_3$, $\text{ACD}=2 \text{ cm}$]

Generally, the bath tended to wet the graphite anode fairly poorly as compared to the cathode [2]. Gas was generated over the entire anode/electrolyte interface during electrolysis. The gas bubbles on the side of the anode varied in size up to about 3 mm and the gas bubble under the anode penetrated a maximum of 5 mm into the electrolyte. With increasing CD, the bubbles became smaller and were formed at a higher frequency. This may be due to the increased amount of gas formed, creating more agitation in the melt.

At higher CDs, coalescence didn't happen as much as at low CDs, and the bubbles escaped before covering the whole anode, as illustrated on Figure 4. The average bubble diameter before release, calculated as the mean diameter of 10 bubbles for each CD, is presented on Figure 5. The diameter decreases from around 18 mm at 0.2 A/cm^2 to 7 mm at 1.6 A/cm^2 . The alumina content in the electrolyte doesn't have a major influence on the bubble size. The release frequency of the CO_2 bubbles is strongly related with the current density.

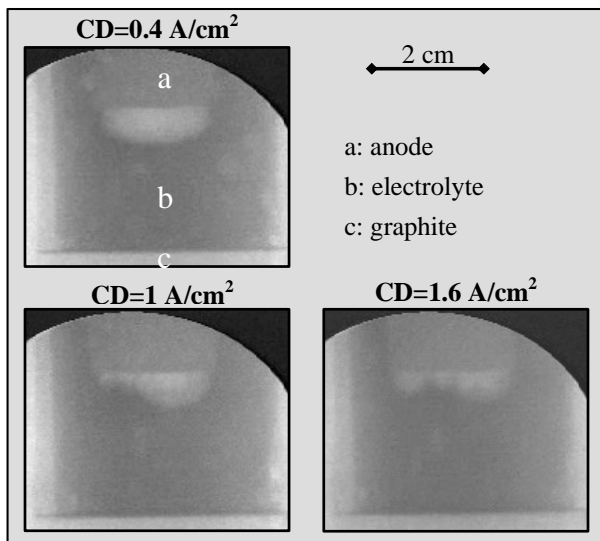


Figure 4: Graphite anode during electrolysis in X-Ray furnace [$\varnothing_{\text{anode}}=18\text{mm}$, $T=960^\circ\text{C}$, $2.5\% \text{ Al}_2\text{O}_3$, $\text{ACD}=2 \text{ cm}$]

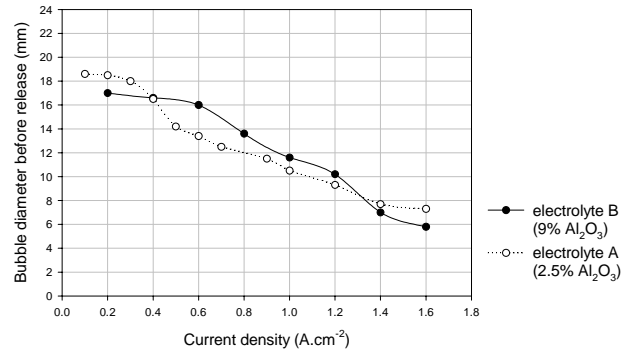


Figure 5: Evolution of average bubble diameter before release under graphite anode [$\varnothing_{\text{anode}}=18\text{mm}$, $T=960^\circ\text{C}$, $\text{ACD}=2 \text{ cm}$]

Using the X-ray technique it was observed that simultaneous with the occurrence of the anode effect, there was a sudden formation of a gas layer under the anode. This sudden non-wetting occurred at the same time as the voltage increased. It was even possible to promote the anode effect using the crucible as the anode. When the anode effect occurred, the melt became separated from the crucible, and a gap of up to 1 mm was observed between the crucible bottom and the electrolyte. Using the hot-stage microscope, electrolysis was carried out with a 1 mm diameter graphite anode. With 10 wt% alumina very fine bubbles form along the anode surface. When only 1 wt% alumina was used, slightly larger gas bubbles formed, and in pure technical cryolite, large bubbles form at the anode indicating poor wetting of the anode. After the anode effect was initiated, the anode became non-wetted and it was difficult to immerse the anode into the electrolyte. It was like pushing a finger into a blown-up rubber balloon with the electrolyte skin stretching around the tip of the anode.

The water modeling study was used to investigate the gas bubble behaviour on a scale similar to that in industry and also to investigate slotted anodes. By the use of a water model, the effects of anode/cathode distance, cathode inclination, and anode gas evolution rate on the mixing rates of electrolyte in the cell could be investigated. The experiments were conducted by filling the tank with water so that the anode was immersed 1 to 15 cm. The gas flowrate, anode angle, and anode-cathode distance were set and blue dye was added at one end of the tank. Five optical sensors were used to measure the light intensity passing through the water from the back to the front of the tank. When the anode was slightly tilted (a fraction of a degree), large bubbles formed and flowed beneath the anode with a leading edge penetrating up to 2 cm into the electrolyte and a long tail as seen in Figure 6. This was also observed by Fortin et al [7] who explained this behaviour by variations in the hydrostatic pressure due to the motion of the bubble. The results are in general agreement with previous researchers [6-8].

When a vertical slot was made in the anode, it was observed that for slots as narrow as 0.5 cm, the moving gas front entered the slot nearly 100%. The gas would flow along the horizontal anode and then up through the slot and leave the anode at its upper side. It was found that even when the slot was fully submerged in the water, as would be the case for anodes just before they have to be

replaced, the gas would flow up into the slot, and then out along the side. For penetration into narrow slots, water and cryolite should behave very similar since the surface tension to density ratio is nearly the same for the two.

Industrially, it is expected that with slotted anodes, gas splashing of cryolite will partly fill and block the upper section of the slots. However, this should not cause any problems since the gas will still be able to escape as seen in this study. Another issue is that the heat up of cold anodes will be more uneven with the center section heated the fastest and initially draw more current than the outer and colder section. On the other hand, for a fully heated anode the current profile through the anode will be more vertical, potentially improving the magnetics of the pot. The reduced gas coverage beneath the anode will lower the cell resistance slightly, but this may be counteracted by a slight increase in the total anode resistance.

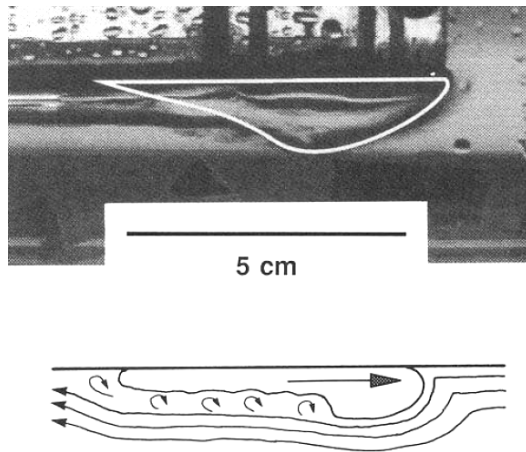


Figure 6: Gas bubble flow behaviour under carbon anode

Bubbling at Inert Anodes

Gas evolution is pretty much the same for tin-oxide, copper and copper-nickel anodes, but was found to be very different as compared to what was observed on the graphite anode. Observations of a tin-oxide anode from above showed tiny bubbles escaping continuously without much coalescence, forming a foam around the electrode, as illustrated in Figure 7. The bubble diameter, measured under the microscope was estimated to be around 0.1 mm, which is 10 to 30 times smaller than on graphite anodes. Some tests were run in see-through cells, but observations were difficult because the froth of bubbles hides the electrode even at small CDs (0.1 A/cm^2). This resulted in poor contrast between the electrolyte and the gas.

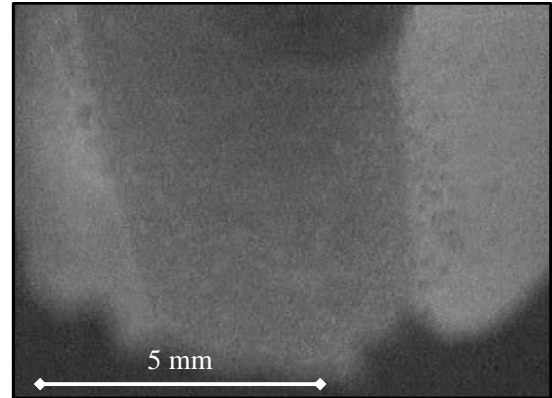


Figure 7: Observation from above - side bubbles on tin-oxide anode [$\varnothing_{\text{anode}}=5\text{mm}$, $\text{CD}=0.2 \text{ A/cm}^2$, $T=960^\circ\text{C}$, 9% Al_2O_3 , $\text{ACD}=2 \text{ cm}$]

Radiographic observation proved to be more adapted to the study of the gas evolution on oxygen evolving anodes. The anode appears in black and the bath in dark grey, while gas takes the form of a light grey halo around and under the electrode (Figure 8). As almost no coalescence occurs between the tiny bubbles, gas release looks continuous, and the gas foam under the electrode keeps roughly a constant shape at fixed CD.

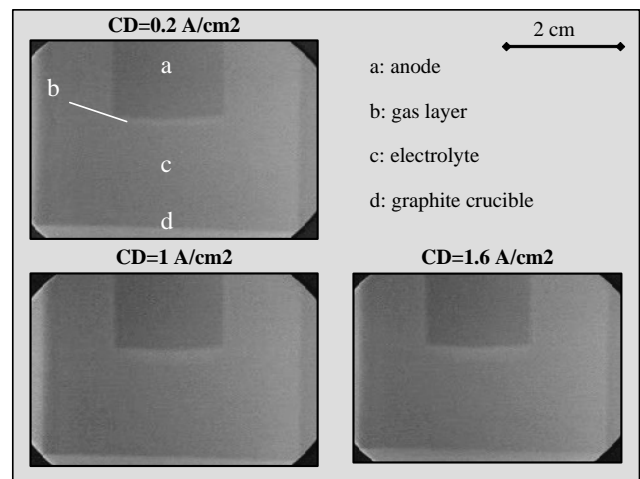


Figure 8: Tin-oxide anode during electrolysis in X-Ray furnace [$\varnothing_{\text{anode}}=18\text{mm}$, $T=960^\circ\text{C}$, 9% Al_2O_3 , $\text{ACD}=2 \text{ cm}$]

The depth of the gas layer under the anode is plotted in Figure 9 as a function of CD and material. The evolution is almost identical for the three oxygen-evolving electrodes: the bubble layer thickness grows regularly with CD until reaching 2-2.5 mm at 1 A/cm^2 . Increasing CD over 1 A/cm^2 doesn't increase the penetration of the gas under the anode, maybe because the volume fraction of the gas in the bubble layer increases. However, the contrast of the X-ray images wasn't good enough to observe noticeable changes in the brightness of the gas froth, as it could be expected with a higher gas density. Another possibility is that the release velocity of the bubbles increases, leading to a shorter residence time of the bubbles under the anode.

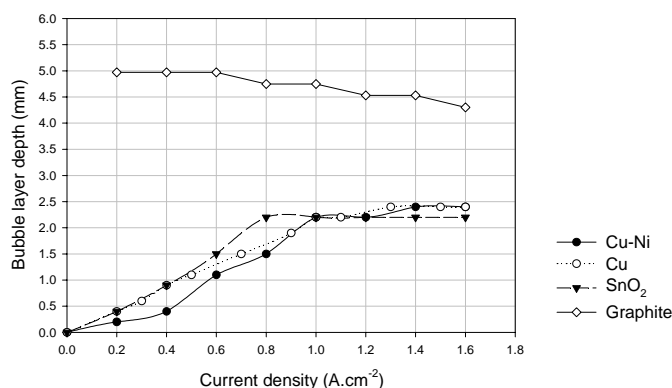


Figure 9: Influence of CD on bubble layer thickness under various anode materials [$\varnothing_{\text{anode}}=18\text{mm}$, $T=960^\circ\text{C}$, $\text{ACD}=2\text{ cm}$]

Test with electrolytes containing either 2.5% or 9% Al_2O_3 on tin-oxide anode didn't reveal any difference in the gas behaviour. The bubble layer under the graphite anode is slightly decreasing with CD from 5 mm to 4.2 mm, confirming both the values and the trend reported by Aaberg et al. [10]. At 1 A/cm^2 , gas penetration under the anode is roughly twice as deep with graphite as with oxygen-evolving anodes, which is important with regards to the anode-cathode optimum distance.

Wetting experiments on graphite versus metallic and tin oxide substrate materials showed that on graphite the electrolyte gave contact angles of about $120\text{-}130^\circ$, indicating poor wetting. However, metallic substrates and tin oxide were completely wetted by the electrolytes forming contact angles of near 0° . This dramatic difference most likely is the reason for the dramatic difference in gas evolution behaviour on graphite versus metallic "inert" anodes. The bubbles formed on tin-oxide, copper and copper-nickel, all very well wetted by the electrolyte, will detach easily from their nucleation site, while bubbles formed on carbon are stuck and grow before detachment.

Conclusions

Video film showing various aspects of the Hall-Héroult process has been developed using X-ray radiography, hot-stage microscopy, direct observations from above the bath and water modeling techniques. During anode effects, the anode is non-wetted by the electrolyte with a thin film surrounding the anode.

Table I. Gas evolution summary

Anodic Material	Bubbling	Bubble diameter	Bubble layer depth
Graphite	Periodic release of large bubbles	2-10 mm	~ 5 mm
Oxygen-evolving	Froth of tiny bubbles	0.1 mm	~ 2 mm

The characterization of the bubble layer under the anode showed many differences between graphite and metallic anodes. The study of three different oxygen-evolving anodes showed that a good wetting by the electrolyte leads to the formation of tiny

bubbles. Contact angle measurements of the system electrolyte-anode-oxygen might then allow predicting the gas evolution on other candidate as inert anodes materials without having recourse to heavy equipment like X-ray radiography.

Water modelling of slotted anodes showed that they are effective in releasing gas bubbles from beneath large anodes. Even narrow slots of about 0.5 cm, allowed for rapid removal of gas as it swept across the surface of the anode.

Acknowledgement

The financial support from the National Science and Engineering Research Counsel of Canada and Pechiney is greatly appreciated.

References

1. L. Cassayre, T.A. Utigard and S. Bouvet, Visualisation of Gas Evolution on Graphite and Oxygen-Evolving Anodes During Aluminum Electrolysis, *Journal of Metals*, 2002, 41-45
2. T.A. Utigard and J.M. Toguri, "Radiographic observations of the Hall-Héroult electrolysis in bench scale cells", in *Bayer and Hall-Héroult Process - Selected Topics*, edited by K. Bielfeldt and K. Grjotheim, Aluminium Verlag, Dusseldorf, Germany, (1988) 133-137.
3. R.P. Pawlek, "Inert anodes: an update", *Light Metals* (2002) 449-456.
4. P. Popelar, T. Utigard and P. Desclaux, "Anode Effect", *Advances in Production and Fabrication of Light Metals and Metal Matrix Composites*, CIM, Annual Meeting, Edmonton, August 1992, 39-54.
5. T.A. Utigard, J.M. Toguri and S.W. Ip, "Direct observation of the anode effect by radiography", *Light Metals* (1988) 703-706.
6. W.E. Haupin and W.C. McGrew, "See-through Hall-Héroult cell", *Aluminum*, 51 (1975) 273-275.
7. S. Fortin, M. Gerhardt, and A.J. Gesing, *Light Metals* (1984) 721-741.
8. B.J. Welch, J.J.J. Chen, W.D. Zhang, J.M. Purdie and M.P. Taylor, "Gas driven electrolyte flow", *Materials Science Forum*, 73-75 (1991) 779-787.
9. A. Solheim and J. Thonstad, "Model cell studies of gas induced resistance in Hall-Héroult cells", *Light Metals* (1986) 397-403.
10. R.J. Aaberg, V. Ranum, K. Williamson and B.J. Welch, "The gas under anodes in aluminium smelting cells Part II: Gas volume and bubble layer characteristics", *Light Metals* (1997) 341-346.